Expanded View Figures

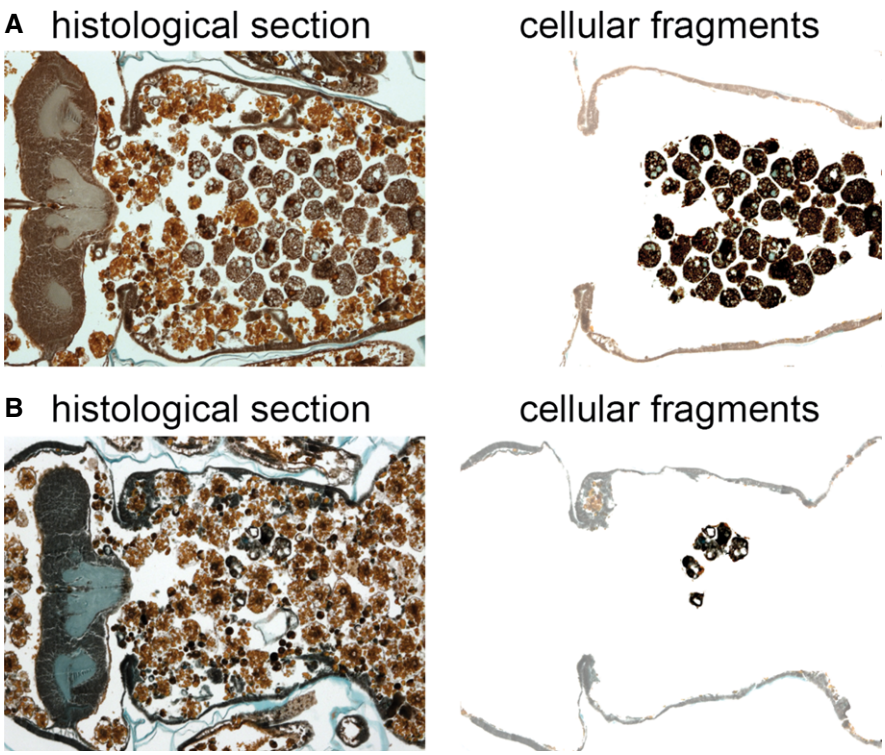

Figure EV1. Description of salivary gland degradation phenotypes observed when Ral is depleted.

A A histological section (left) 24 h after puparium formation of an animal with a strong salivary gland degradation defect (*fkh*-GAL4/*ω*; UAS-*ral*^{IR}/+). The salivary glands are partially degraded with many cellular fragments remaining. The persistent salivary gland tissue has been highlighted by removal of the surrounding tissues (right).

B A histological section (left) 24 h after puparium formation of an animal with a weak salivary gland degradation defect (*ral*^{35D}/Y). The salivary glands are mostly degraded, but a few cellular fragments persist (this time point is 8 h after salivary glands would fully degrade in a wild-type animal). The remaining salivary gland tissue has been highlighted by removal of the surrounding tissues (right).

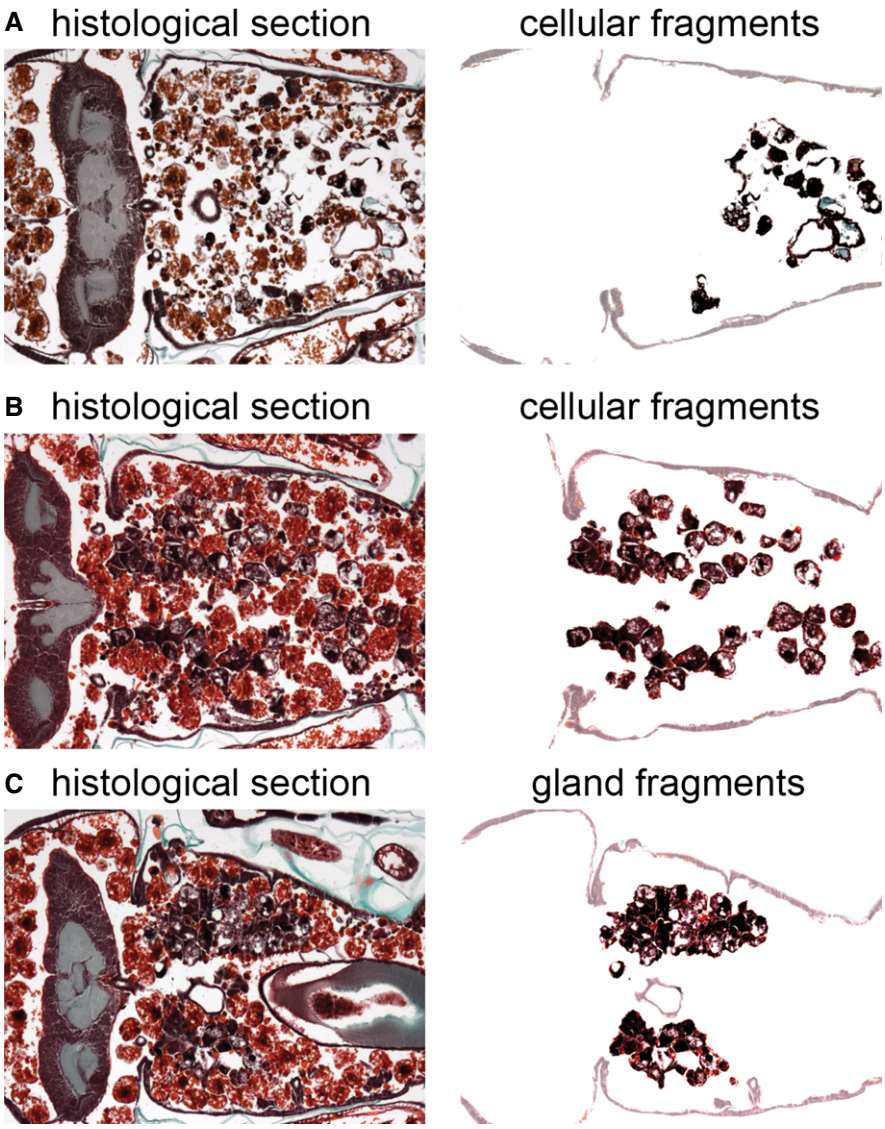

Figure EV2. Description of salivary gland degradation phenotypes.

A, B Histological sections (left) 24 h after puparium formation of animals with partially degraded salivary glands resulting in a cellular fragment phenotype (A) ral^{35d}/Y; UAS-p35/+, (B) ral^{35d}/+; UAS-p35/*fkh*-GAL4. The remaining salivary gland tissue has been highlighted by removal of the surrounding tissues (right). Note the diffuse nature of the persistent salivary gland material.

C A histological section (left) 24 h after puparium formation of an animal with partially degraded salivary glands resulting in a gland fragment phenotype (ral^{35d}/Y; UAS-p35/*fkh*-GAL4). The remaining salivary gland tissue has been highlighted by removal of the surrounding tissues (right). Note that the remaining salivary gland tissue retains its basic glandular structure and is less diffuse than in (A) or (B).

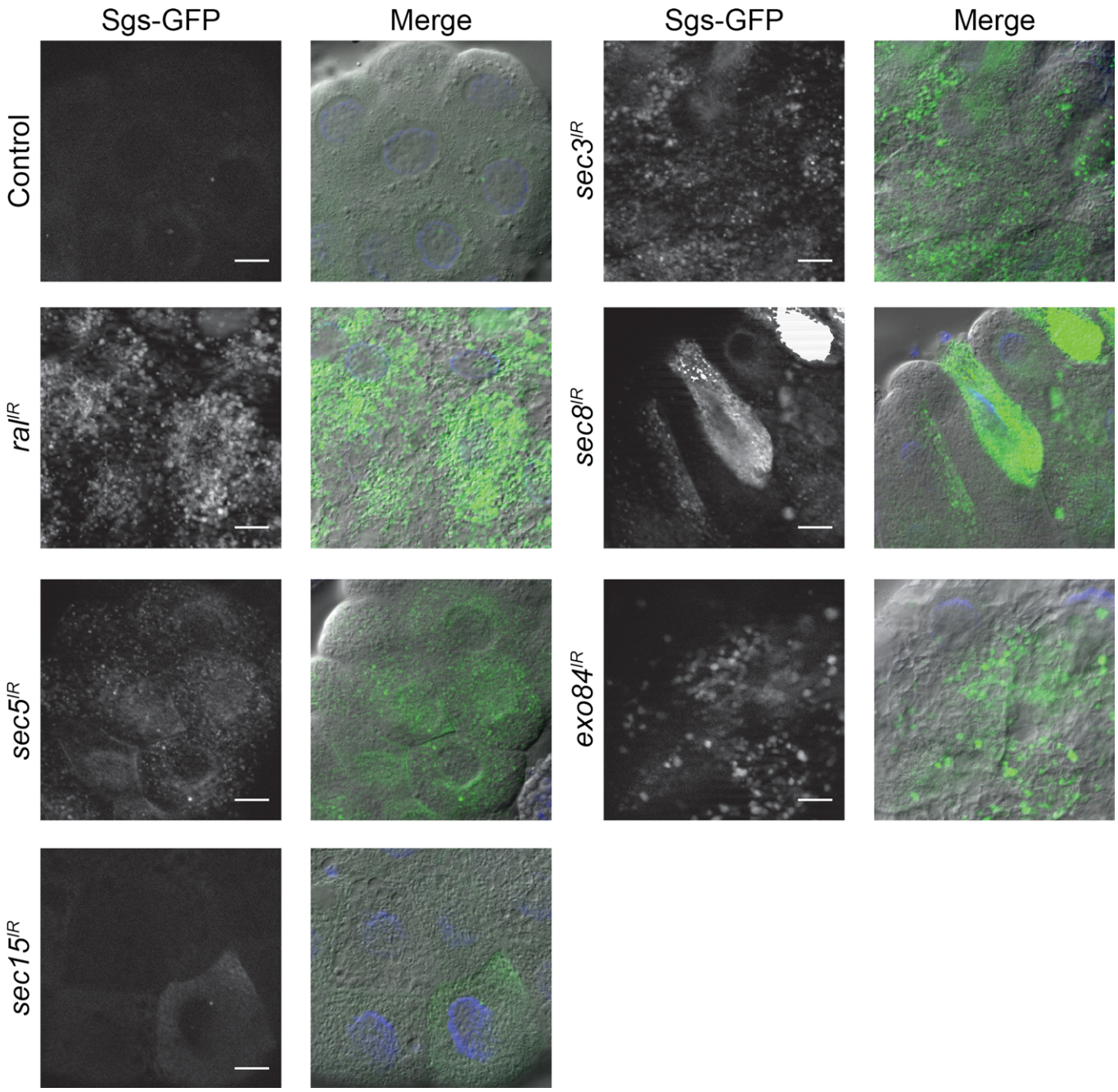

Figure EV3. Ral and the exocyst are required for protein secretion in salivary glands.
At the end of larval development, the salivary gland cells secrete a large amount of glue proteins in response to steroid signaling, and the glue is extruded at pupariation (0 h after puparium formation). Exocytosis of the glue proteins can be monitored *in vivo* using a transgenic fusion of the secreted glue protein, Sgs3, and GFP. Here, salivary glands dissected from 6 h after puparium formation control animals (*fkh*-GAL4/+; *SgsΔ3*-GFP/+), and those with salivary gland-specific knockdown of *ral* (*fkh*-GAL4/*w*; *SgsΔ3*-GFP/+; UAS-*ral*^{IR}/+), *sec5* (*fkh*-GAL4/*w*; *SgsΔ3*-GFP/+; UAS-*sec5*^{IR}/+), *sec15* (*fkh*-GAL4/*w*; *SgsΔ3*-GFP/+; UAS-*sec15*^{IR}/+), *sec3* (*fkh*-GAL4/*w*; *SgsΔ3*-GFP/UAS-*sec3*^{IR}), *sec8* (*fkh*-GAL4/*w*; *SgsΔ3*-GFP/UAS-*sec8*^{IR}), *exo84* (*fkh*-GAL4/*w*; *SgsΔ3*-GFP/UAS-*exo84*^{IR}) were analyzed for the presence of *SgsΔ3*-GFP. The merged images are GFP (green), Hoescht (blue), and DIC. Scale bars represent 20 μm.

Figure EV4. Inhibiting the exocyst does not induce ectopic autophagy in fat bodies.

A, B Fat body dissected from feeding larvae expressing eGFP-Atg8a in all cells and ral^{IR} specifically in dsRed-marked clone cells (hsflp/*w*; peGFP-Atg8a/+; *act* < FRT, cd2, FRT > GAL4, UAS-dsRed/+) analyzed for eGFP-Atg8a puncta. Quantification of the data is shown in (B).

C–L Fat bodies dissected from feeding larvae expressing mCherry-Atg8a in all cells, and (C) $sec5^{IR}$, (E) $sec15^{IR}$, (G) $sec3^{IR}$, (I) $sec8^{IR}$, (K) $exo84^{IR}$ specifically in GFP-marked clone cells (hsflp/*w*; pmCherry-Atg8a/+; *act* < FRT, cd2, FRT > GAL4, UAS-GFP/+) analyzed for mCherry-Atg8a puncta. Quantification of the data from (C, E, G, I, K) is shown in (D, F, H, J, L), respectively.

Data information: Scale bars represent 20 μm. Data are represented as means ± SEM; $n \geq 10$. Statistical significance was determined using a Student's *t*-test.

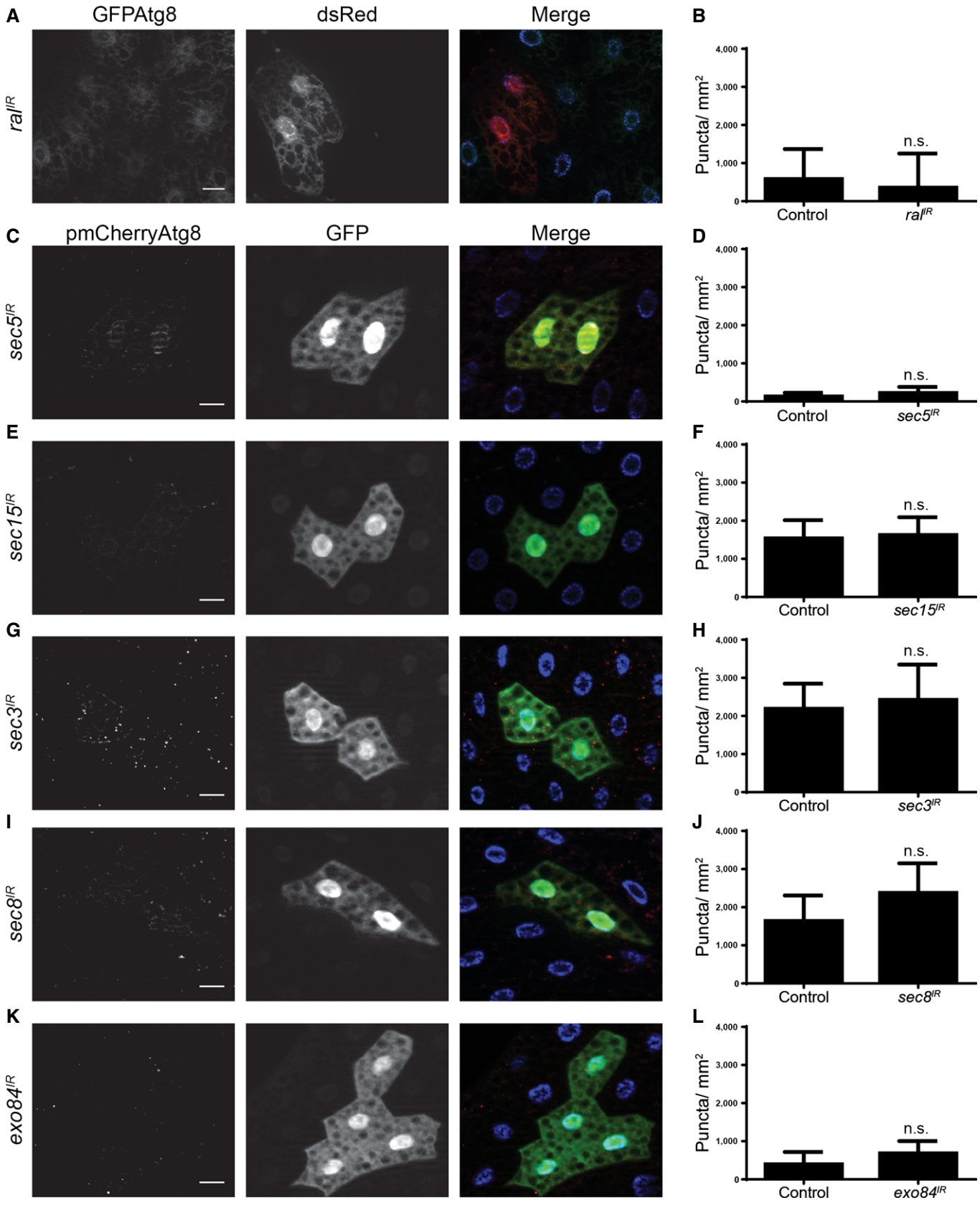

Figure EV4.